

## ETSA and RAMAC GPR DATA OBTAINED AT LSBB – A COMPARATIVE STUDY

Matthew Yedlin<sup>1</sup> ([matty@ece.ubc.ca](mailto:matty@ece.ubc.ca)), Guy Sénéchal<sup>2</sup>, Dominique. Rousset<sup>2</sup>, Nicolas Fortino<sup>3</sup>, Jean-Yves Dauvignac<sup>3</sup>, Stéphane Gaffet<sup>4,5</sup>, Tony Monfret<sup>4</sup>, and Christian Pichot<sup>3</sup>

1. University of British Columbia, Vancouver, BC, Canada
2. MIGP, Université de Pau et des Pays de l'Adour, Pau, France
3. LEAT, University of Nice-Sophia Antipolis, CNRS, Valbonne, France
4. GEOAZUR, UNS/CNRS/OCA, Valbonne, France
5. LSBB, UNS/CNRS/OCA, Rustrel, France

**Keywords:** Ultra-wideband, ground penetrating radar, Stockwell transform

### ABSTRACT

A comparison is made between two GPR (ground penetrating radar) systems – one a conventional RAMCA 250 MHz bistatic system and a new bistatic UWB (Ultra-wideband) system with a bandwidth from 130 MHz to 2000 MHz. The data collected for this comparison was obtained in the floor of the anti-blast tunnel (GAS) at LSBB (<http://lsbb.oca.eu>), which is situated in a karst aquifer.

### INTRODUCTION

In the current study we compare data obtained using a MALÅ Geosciences 250 MHz RAMAC system, which employs omnidirectional, narrowband antennas, with the novel UWB system. The UWB system employs Exponentially Tapered Slot Antennas (ETSA), with a usable bandwidth from 130 MHz to 2.0 GHz connected to an Agilent PNA (Precision Network Analyzer) with a noise floor of -120 dB. The PNA creates a synthetic pulse via a stepped frequency algorithm. The recorded amplitudes and phases of the reflection and transmission coefficients ( $S_{11}$  and  $S_{21}$  parameters) are filtered and inverse Fourier transformed to obtain the time-domain data. Due to the very low noise floor a wider dynamic range is available. In addition, due to the large bandwidth, enhanced resolution is obtained at depth

### MEASUREMENT PROCEDURE

The bistatic UWB GPR system is based on the exponentially tapered slot antenna (ETSA) developed at LEAT. A picture of this antenna is shown in Fig.1. The copper ground plane, in the shape of a whale, is clearly visible. The antenna itself is balanced and consists of two ground planes and one radiating plane. The antenna dimensions are 0.8 m by 0.8 m.

Both antenna systems were displaced a distance of 20 m in the anti-blast tunnel. The RAMAC system was moved in 10 cm increments while the UWB system was displaced in 5 cm increments. RAMAC data was recorded directly in time, while the UWB system was recorded in frequency, with a frequency interval of 62.5 KHz, over the entire bandwidth. Minimization of noise interference was accomplished by using a 0.5 ton carriage containing ultra-wideband absorbing material and by using low noise and low loss cables.



Fig. 1: ETSA antenna with exterior ground plane visible.

The carriage prevented coupling between the transmitting and receiving antennas and also reflections from the ceiling and walls of the tunnel.

### DATA PROCESSING

Before comparing the data directly in time, the frequency data of the UWB system was inverse Fourier-transformed and then resampled to the same time sampling of 0.4 ns as used by the RAMAC system.

For both datasets, Seismic Unix was used to perform all data processing. The resultant time-sections for both data sets had strong, shallow horizontal ringing which had to be removed. However, before this removal, both raw datasets were bandpass filtered using a band from 200 to 650 MHz. Then the mean-trace was calculated and subtracted from the entire time section. This removal will of course eliminate any horizontal reflections from subsurface impedance contrasts. Structural mapping in the tunnel indicates, however, that there is no dominant horizontal bedding.

Deep reflection events in the time sections are difficult to observe unless a time-varying gain function is applied. After some experimentation, we found that a data-driven gain correction provided the best dynamic range. This gain correction was applied by first computing the envelope of each trace in order to obtain the mean envelope. The data was then divided by this mean envelope. Low frequency artifacts were removed

by high-pass filtering. In the ETSA data, anomalously high, narrow-band ranging was removed via a sequence of notch filters. The processed data are shown in Fig. 2 (RAMAC) and Fig. 3 (ETSA).

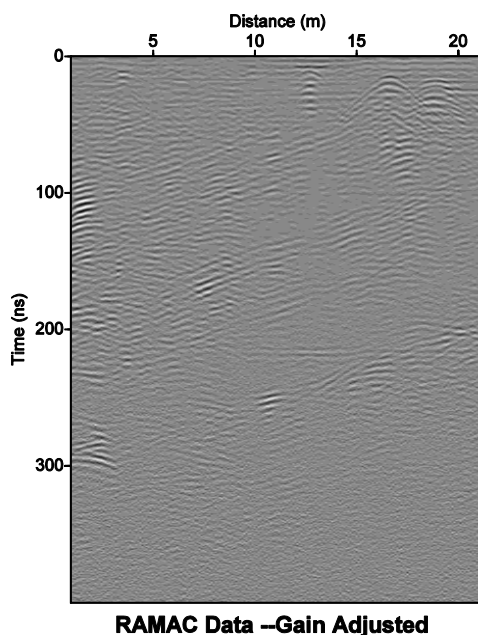


Fig. 2: RAMAC Gain Adjusted Data

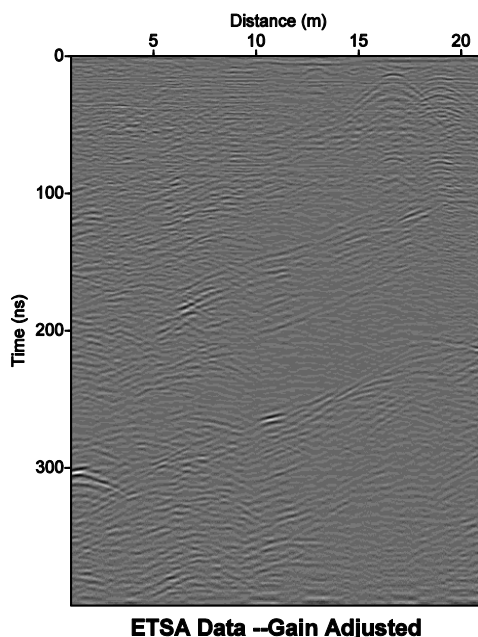


Fig. 3: ETSA Gain Adjusted Data

Comparison of figures 2 and 3 indicates that the two data sets are very similar. There are however two obvious differences. First, the ETSA time section has coherent arrivals below 300 ns that are not visible in the RAMAC time section. Second the data are non-linearly time-shifted in the RAMAC data as compared to the ETSA data. This shift is clearly visible if we compare the hyperbolic arrival at 0 m and near 300 ns.

## TIME-FREQUENCY ANALYSIS

In order to quantify the frequency content as a function of time, the Stockwell transform [1] given by

$$S(b, \xi) = \int_{-\infty}^{\infty} f(x) |\xi| \frac{e^{-\frac{(x-b)^2 \xi^2}{2}}}{\sqrt{2\pi}} e^{-2\pi i \xi x} dx \quad (1)$$

is applied to the ETSA data at trace 1 containing the hyperbolic arrival at 300 ns.

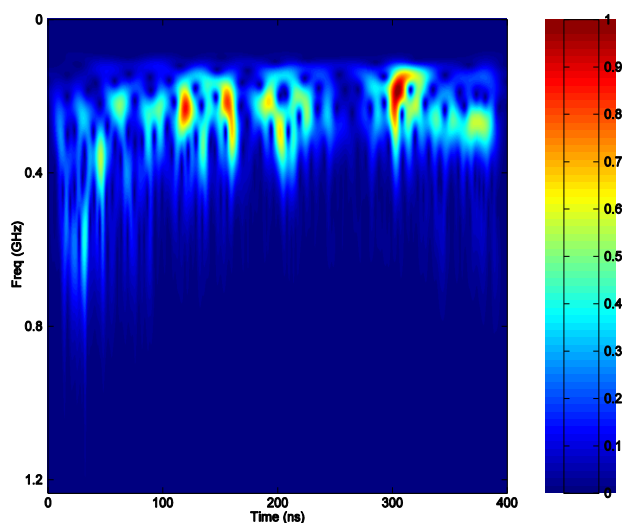


Fig. 4: Stockwell Transform Amplitude for Trace 1

In Fig. 4, the normalized amplitude of the Stockwell transform of the first trace at 0 m is presented. Clearly visible is the frequency content of the hyperbolic arrival near 300 ns.

## CONCLUSION

The results of the data collected by two different GPR systems – a RAMAC 250 MHz bistatic narrowband omnidirectional system and a stepped frequency UWB system show similar features. However, the UWB system has better resolution and less noise at later times. The nonlinear stretching of the RAMAC data relative to the UWB data is currently being investigated. Application of the Stockwell transform to the data offers an excellent possibility for quantification of the frequency content as a function of time.

## REFERENCES

- [1] Stockwell, R. G., Mansinha L. and Lowe, R. P., 1996. Localization of the complex spectrum: the *S* transform, *IEEE Trans. on Signal Processing*, **44**, 998-1001.